frontiers | Frontiers in Marine Science

TYPE Original Research
PUBLISHED 14 January 2026
DOI 10.3389/fmars.2025.1751567

EDITED BY
Xianbiao Lin,
Ocean University of China, China

REVIEWED BY
Yuan Bo,
Xi'an University of Science and Technology, China
Niu Li,
Chinese Academy of Forestry, China

*CORRESPONDENCE
Jiafang Huang
wahugeo@fjnu.edu.cn

RECEIVED 21 November 2025
REVISED 05 December 2025
ACCEPTED 10 December 2025
PUBLISHED 14 January 2026

CITATION
Gao D, Zhang Y and Huang J (2026) Inundation mitigates the nitrogen-induced increase in soil nitrous oxide emissions in estuarine and coastal wetlands.
Front. Mar. Sci. 12:1751567.
doi: 10.3389/fmars.2025.1751567

Inundation mitigates the nitrogen-induced increase in soil nitrous oxide emissions in estuarine and coastal wetlands

Dengzhou Gao[1,2], Yixiao Zhang[1] and Jiafang Huang[1*]

[1]Key Laboratory of Humid Subtropical Eco-geographical Process of Ministry of Education, College of Geographical Sciences, Fujian Normal University, Fuzhou, China, [2]State Key Laboratory of Estuarine and Coastal Research, East China Normal University, Shanghai, China

Nitrogen enrichment and sea-level rise are two critical drivers affecting estuarine and coastal wetland ecosystems globally. However, the effects of these drivers on soil nitrous oxide (N_2O) production, consumption, and resulting ultimate emissions remain poorly understood. In this study, nitrogen input (+N treatment), increased inundation (+I treatment), and their combination (+N+I treatment) were simulated *in situ* using a weir device to explore the individual and interactive effects of enhanced nitrogen loading and sea-level rise on soil N_2O dynamics. Our results showed that nitrogen input (+N treatment) significantly increased soil N_2O emission (82.9%), primarily by stimulating gross N_2O production. In contrast, the inundation increases alone (+I treatment) did not alter soil N_2O production and consumption process dynamics. The Combined treatment of increased nitrogen input and inundation (+N+I treatment) dramatically promoted soil gross N_2O production (85.3%). However, an elevated proportion of N_2O consumption mitigates its effect on N_2O emissions. This implies that increased inundation resulting from the sea level rise may counteract nitrogen-stimulated soil N_2O emissions. The contents of soil carbon and nitrogen substrate (e.g., DOC and NH_4^+), along with the gene abundances (e.g., nosZ) involved in N_2O production and consumption, were the pivotal factors in mediating the changes in N_2O dynamics under various treatments. Overall, our findings highlighted the importance of increased inundation caused by sea-level rise in alleviating N_2O emissions under high nitrogen conditions, yet widely overlooked.

KEYWORDS

emission dynamics, estuarine wetland, nitrogen enrichment, nitrous oxide, sea-level rise

1 Introduction

Nitrous oxide (N_2O) is a significant trace gas that can aggravate the greenhouse effect and deplete stratospheric ozone (Ravishankara et al., 2009; IPCC, 2021). N_2O concentrations in the atmosphere have risen by 20% since the beginning of the industrial revolution and are still increasing by approximately 0.73 ± 0.03 ppb per year

(Toyoda et al., 2017; Wang et al., 2023). It is estimated that about 57% of atmospheric N_2O is derived from the nitrogen biogeochemical processes occurring in natural ecosystems (Tian et al., 2020; Bi et al., 2024). Herein, estuarine and coastal zones are widely recognized as hotspots for nitrogen transformations and important sources of N_2O in the atmosphere (Murray et al., 2015; Li et al., 2023; Yang et al., 2024). Therefore, N_2O emission dynamics and their influencing mechanisms in estuarine and coastal wetlands have received much attention over the last decades.

Nitrogen loading enhancement is an urgent environmental issue in estuarine and coastal ecosystems, disturbing the inherent nitrogen biogeochemical balance and N_2O emission dynamics (Lenstra et al., 2021; Zhang et al., 2023). To date, extensive studies have been conducted on the impacts of elevated nitrogen loading on N_2O emissions/fluxes in estuarine and coastal areas, which consistently concluded that nitrogen enrichment remarkably facilitates N_2O emissions/fluxes (Zhang et al., 2013; Wankel et al., 2017; Martin et al., 2018; Quick et al., 2019; Peng et al., 2021; Li et al., 2023). Nevertheless, N_2O emission is fundamentally determined by the balance between its gross production and consumption (Gao et al., 2022). So far, it is still unclear how nitrogen enrichment affects gross N_2O production and consumption to facilitate ultimate N_2O emission. Sea-level rise, as a result of global warming, is another important factor affecting estuarine and coastal ecosystems (Saintilan et al., 2020; Lorenz et al., 2023). In recent years, numerous works have also explored the effects of sea-level rise on element biogeochemical processes, but they mainly focused on organic carbon decomposition and mineralization (Lewis et al., 2014; Stagg et al., 2017; Liu et al., 2022). These studies showed that the impacts of sea-level rise on carbon cycles exhibit variability, with the potential for positive, negative, or neutral outcomes. Generally, the changes in salinity, water content, and gaseous diffusion ability caused by sea-level rise were found to be important factors affecting organic carbon dynamics (Jones et al., 2018; Luo et al., 2019), which may also alter N_2O emissions/fluxes. Nevertheless, the changes in N_2O emission dynamics in estuarine and coastal ecosystems under a sea-level rise scenario are not well understood.

In addition, nitrogen loading enhancement and sea-level rise often occur simultaneously in estuarine coastal wetlands (Liu et al., 2022), which would further complicate N_2O dynamics. Thus, it is crucial to develop the capability to predict N_2O emission dynamics in relation to these multiple factors. However, understanding N_2O dynamics based on multiple influencing factors is not that straightforward due to potential additive and/or non-additive effects (Dieleman et al., 2012; Luo et al., 2019). For instance, Li et al. (2019) reported that increased salinity significantly stimulated N_2O emission by promoting nitrogen transformation rates and organic carbon decomposition. By contrast, in nitrogen addition experiments, salinity reduced the response size of N_2O emission to nitrogen enrichment (Jia et al., 2020). Despite extensive studies, the factors that regulate N_2O emission dynamics remain underexplored, specifically, the knowledge of how sea-level rise influences nitrogen-induced increases in N_2O emissions is still very limited. Therefore, understanding the response of N_2O dynamics to nitrogen enrichment and sea-level rise, as well as their interactions, will be crucial for Earth system models to precisely evaluate the N_2O budget and associated climate feedback driven by these two global change drivers.

The multi-factor studies on soil N_2O emission dynamics in estuarine and coastal wetlands were mainly based on laboratory simulation due to the *in-situ* technical and logistical challenges (Wankel et al., 2017; Li et al., 2019; Jia et al., 2020). To this end, Cherry et al. (2015) developed an approach named weir design, which not only can effectively reflect sea-level rise but also perform nutrient addition with minimal cross-contamination effects. After that, the weir approach has also been widely applied in multi-factor influence studies in estuarine and coastal wetlands (Stachelek et al., 2018; Martin et al., 2021; Liu et al., 2022). Here, nitrogen input, inundation increase, and their interactions were simulated *in situ* based on a weir device to explore the changes in soil N_2O emission dynamics in estuarine and coastal wetlands in the context of nitrogen loading enhancement and/or sea-level rise. The main objectives of this study were to (1) investigate the effects of nitrogen input, inundation increase, and their interactions on soil N_2O emission rates; (2) reveal how nitrogen input and inundation increase regulate gross N_2O production and consumption by interacting with ancillary geochemical variables and microbial abundances; and (3) assess relevant environmental implications of N_2O emissions in estuarine and coastal wetlands experiencing nitrogen loading enhancement and sea-level rise, and provide the scientific basis for the management in such ecosystems.

2 Materials and methods

2.1 Study area and experimental design

The study site was located in Shanyutan (119°34′12″ – 119°40′40″E, 26°00′36″ – 26°03′42″N), the largest intertidal wetland in the Min River Estuary, Southeast China. This area belongs to a subtropical monsoon climate, with 19.6°C for the annual average temperature and 1350 mm for the annual average rainfall (Zhang et al., 2015). The tide in the Min River Estuary is irregularly semidiurnal with average tidal amplitudes of 4.1 m. The wetland exhibits a high richness of plant species, with the dominant native marsh species being *Phragmites australis*, *Cyperus malaccensis*, and *Scirpus triqueter* (Gao et al., 2017). The site is characterized by coastal saline soil, with a particle size distribution of 62–78% silt, 19.05–37.39% clay, and 0.28–4.77% sand (Zhang et al., 2015). This experimental site was situated in a pure *C. malaccensis* habitat in the central-western region of the Shanyutan wetland. The study area experiences a regular semi-diurnal tide, and the experimental site is submerged for approximately 5 hours within a 24-hour cycle (Liu et al., 2022).

The *in situ* simulation experiment consisted of four treatments: control treatment (Control), nitrogen input treatment (+N), inundation increase treatment (+I), and combined nitrogen input and inundation increase treatment (+N+I), with three replicates for each treatment. The nitrogen input and inundation increase were used to characterize nitrogen loading enhancement and sea-level rise, respectively (Cherry et al., 2015; Liu et al., 2022). At the study site, twelve plots (1 m × 1 m) were randomly assigned to the four treatments mentioned above. To minimize any cross-influence, the distance between adjacent treatments was set at approximately 3 m. Previously, Cherry et al. (2015) developed a novel method using weirs to simulate inundation increases caused by sea-level rise *in situ* at relatively large spatial scales. In the present study, the weir device used for +I and +N+I treatments was improved by equipping the in-line check valve and floating ball valve, and this modification allowed for more flexibility in regulating the duration of inundation. In the control and +N treatments, the weir had only a hole and lacked an in-line check valve or float ball valve, allowing tidal water to flow naturally through the weir. Liu et al. (2022) provided a more detailed description of the weir device. The weir had a height of 100 cm, with 30 cm being pressed into the soil. Our investigation showed that the duration of inundation in the +I and +N+I treatments was approximately 1.5 times and 3 times compared to the control and +N treatments in summer and winter, respectively (Liu et al., 2022).

The *in situ* simulation experiments were started in November 2018. For the +N and +N+I treatments, the annual nitrogen input was approximately 48 g m^{-2}, which was approximately 2 times the total nitrogen import amount in the Min River Estuary (Ti and Yan, 2010; Mou et al., 2014). Nitrogen was supplied in the form of NH_4^+-N (as NH_4Cl) and NO_3^--N (as $NaNO_3$) at a ratio of 1:2 based on the nitrogen wet deposition in our study area (Liu et al., 2022). The mixed solution of NH_4Cl and $NaNO_3$ was sprayed into the weir biweekly. In detail, a certain amount of NH_4Cl (2.5 g) and $NaNO_3$ (8.1 g) are first dissolved in 2 L of tidal water and slowly sprayed on the soil surface of the weir. Subsequently, an additional 2 L of tidal water was sprayed again to wash the plants. To decrease the error in the experimental system, the weirs in control and +I treatments were also sprayed with 4 L of tidal water. The spray of nitrogen solutions/tidal water was carried out after the ebb of the neap tide to maximize the retention of the added solution/tidal water within the weir (Moseman-Valtierra et al., 2011; Hu et al., 2016).

2.2 Soil and porewater samples collection

The surface soil (0–10 cm) was collected from each weir on days 240 (July 2019), 420 (January 2020), and 630 (August 2020) of the experiment using a 5-cm diameter steel soil sampler. After removing plant residues, roots, and recognizable stones, the soil samples were placed in sterile ziplock bags. Meanwhile, the Rhizon pore water sampler was used to collect pore water at 0 – 10 cm depths of soil (Hu et al., 2016). Subsequently, the porewater sample was transferred into a 100 mL sterile centrifuge tube, and the saturated mercuric chloride solution (0.2 mL) was added to terminate microbial activities (Liu et al., 2022). Then, soil and porewater samples were stored in a cooler at approximately 4°C and returned to the laboratory within 6 h. In the laboratory, soil samples were homogenized and separated into two parts: one part was stored at 4°C to determine geochemical properties and N_2O dynamics, and the second part was frozen at -80°C to extract DNA. Porewater samples were filtered via 0.22-µm cellulose membrane filters (Millipore, USA) and used to analyze dissolved organic carbon (DOC), ammonium (NH_4^+), and nitrate (NO_3^-).

2.3 Analysis of soil and porewater characteristics

Soil temperature and pH were determined *in situ* by using a hand-held pH meter (pH400 instrument, Spectrum Technologies Inc., USA). The salinity in the soil was measured by the portable salinity meter (YSI-30, USA). Soil bulk density and water content were analyzed by the cutting-ring method and oven-drying method, respectively (Zhang et al., 2015). Total organic carbon (TOC) and total nitrogen (TN) of soil were measured using an elemental analyzer (Elementar Vario MAX CN, Germany) after acid pickling (1 M HCl). The ferrozine method was used to measure the total extractable iron (Fe) and ferrous iron (Fe(II)), and the ferric iron (Fe(III)) was calculated by the Fe minus Fe(II) (Kostka and Luther, 1994). Porewater DOC concentration was measured by a total organic carbon analyzer (TOC-V CPH, Shimadzu, Japan) (Li et al., 2022). The automatic flow injection analyzer (Skalar Analytical SAN++, the Netherlands) was used to analyze porewater NH_4^+ and NO_3^- concentrations (Zhang et al., 2014).

2.4 DNA extraction and quantitative PCR

The total genomic DNA was extracted from 0.25 g of homogenized soil using Powersoil ™ DNA Isolation Kits (MOBIO, USA) following the manufacturer's instructions. Eight microbial nitrogen cycling genes (AOA *amoA*, AOB *amoA*, *hao*, *nxrB*, *narG*, *nirK*, *nirS*, and *nosZ*) associated with N_2O production and consumption processes were quantified using q-PCR analysis with an ABI7500 Sequence Detection System. Detailed information about primers and thermal conditions for qPCR is shown in Supplementary Table S1. These gene copy numbers were calculated based on the standard curves, which were constructed by a 10-fold dilution series of standard plasmids. In this work, the amplification efficiencies for targeted genes were above 90%, and the correlation coefficient was higher than 0.98.

2.5 Determination of N_2O dynamics

N_2O dynamics (net N_2O emission rates, gross N_2O production rates, and gross N_2O consumption rates) were analyzed based on the C_2H_2 inhibition methods following the procedure as described by Lin et al. (2022). For each sample, nine 125 mL serum bottles were filled with approximately 30 g of fresh soil. Then, all serum bottles were flushed with high-purity air in an enclosed glove box to eliminate background N_2O and sealed with a butyl stopper. Three headspace treatments were conducted for each soil sample with three replicates: 10 kPa of C_2H_2 (N_2O reduction and nitrification were inhibited), 10 Pa of C_2H_2 (nitrification was inhibited), and 0 Pa of C_2H_2 (net N_2O emission). Here, 10 mL headspace gas in serum bottles was replaced with the same amount of air-diluted C_2H_2 to reach the target concentration of C_2H_2. Meanwhile, the 0 Pa of C_2H_2 treatments were also replaced with the same amount of high-purity air. After incubation at near *in situ* temperature for 12 h, the headspace gas samples were collected with gastight syringes, and gas chromatography (GC-2014, Shimadzu, Kyoto, Japan) was used to measure N_2O concentrations. The net N_2O production rates under 10 kPa ($R_{10\ kPa}$), 10 Pa ($R_{10\ Pa}$), and 0 Pa ($R_{0\ Pa}$) C_2H_2 treatments were calculated as follows (Equation 1) (Yin et al., 2020):

$$R_{10\ kPa}(R_{10\ Pa}\ or\ R_{0\ Pa}) = \frac{dc}{dt} \times \frac{V_h}{M_s} \times \frac{M_w}{M_v} \times \frac{T_{st}}{T_{st} + T} \quad (1)$$

where $R_{10\ kPa}$, $R_{10\ Pa}$ and $R_{0\ Pa}$ (nmol g^{-1} h^{-1}) denote net N_2O production rates under 10 kPa, 10 Pa and 0 Pa C_2H_2 treatments; $\frac{dc}{dt}$ (μL L^{-1} h^{-1}) is the change in N_2O concentrations inside the bottles during the 12 h incubation; V_h (L) represents the headspace volume of the incubation bottle, and M_s (g) denotes the weight of soil. M_w (g mol^{-1}) and M_v (L mol^{-1}) are the molecular weight and volume of N_2O, respectively. T (°C) and T_{st} (K) represent incubation temperature and standard temperature, respectively. The Equations 2–5 were used to estimate net N_2O emission rates ($N_2O_{Net\ emission}$), gross N_2O production rates ($N_2O_{Gross\ production}$), gross N_2O consumption rates ($N_2O_{Gross\ consumption}$), and N_2O consumption proportions ($N_2O_{Consumption\ proportion}$) (Yin et al., 2020; Lin et al., 2022).

$$N_2O_{Net\ emission} = R_{0\ Pa} \quad (2)$$

$$N_2O_{Gross\ consumption} = R_{10\ kPa} - R_{10\ Pa} \quad (3)$$

$$N_2O_{Gross\ production} = R_{10\ kPa} - R_{10\ Pa} + R_{0\ Pa} \quad (4)$$

$$N_2O_{Consumption\ proportion} = \frac{R_{10\ kPa} - R_{10\ Pa}}{R_{10\ kPa} - R_{10\ Pa} + R_{0\ Pa}} \times 100\,\% \quad (5)$$

2.6 Statistical analyses

The data were examined for normality and the need for any necessary transformations before statistical analysis. All analysis was conducted using R 4.3.1 software. The effects of nitrogen input, inundation increase, and their interactions on soil and porewater geochemical properties, microbial gene abundances, and N_2O dynamics were tested by two-way ANOVA based on the 'aov' function. Tukey's HSD *post hoc* test was used to determine multiple comparisons among different treatments on the same sampling date. The Pearson correlation and redundancy analysis (RDA) were used to explore the effects of soil geochemical properties and microbial gene abundances on N_2O dynamics. Random forest analyses (RF) were conducted to identify the statistically significant predictors of N_2O dynamics using the 'linkET' package (Feng et al., 2021). We compared the proportion increases in the mean squared error (MSE) to identify the relative importance of geochemical properties and microbial gene abundances in predicting N_2O dynamics.

3 Results

3.1 Geochemical properties of soil and porewater

The soil temperature at 240 d (Jul. 2019), 420 d (Jan. 2020) and 630 d (Aug. 2020) varied from 27.57 – 27.67°C, 15.50 – 15.77°C and 30.40 – 31.23°C, respectively, but there were no significant differences among the treatments on the same sampling date (Figure 1i, Supplementary Table S2). Soil water content, bulk density, pH and salinity were in the range of 37.19 – 56.39%, 0.59 – 0.98 g cm^{-3}, 5.48 – 7.14 ‰ and 2.23 – 5.60 ‰, respectively, and the +N, +I, and +N+I treatments generally did not alter these physicochemical parameters (Figures 1ii–v; Supplementary Table S2). The water content and pH of soil were observably lower at 630 d (Aug. 2020) as compared to 240 d (Jul. 2019) and 420 d (Jan. 2020), but the opposite was true for bulk density. Soil salinity at 420 d (Jan. 2020) was significantly higher than that at 240 d (Jul. 2019) and 630 d (Aug. 2020) (Figure 1v). The TOC and TN contents of the soil varied from 16.63 – 37.20 mg g^{-1} and 1.71 – 3.09 mg g^{-1}, respectively, and the +N and +N+I treatments generally increased their values compared to the control treatment, except at 420 d (Jan. 2020) (Figures 1vi, vii). Soil Fe(II) contents in the +N treatment were higher than those in other treatments, but no significant differences were observed for Fe(III) contents among the four treatments (Figures 1viii, ix; Supplementary Table S2). Porewater DOC concentration ranged from 14.48 – 57.22 mmol L^{-1}, which was lowest in the control treatment, followed by the +I and +I+N treatments, and highest in the +N treatment (Figure 1x). The +N and +N+I treatments generally increased porewater NH_4^+ concentrations, but they were comparable between the +I and control treatments (Figure 1xi). The NO_3^- concentrations of porewater were also higher in the +N and +I+N treatments (1.35 – 5.77 μmol L^{-1}), and no significant differences were observed between +I and control treatments (0.97 – 3.39 μmol L^{-1}) (Figure 1xii).

3.2 Soil gene abundances

The +N and +I+N treatments generally increased AOA-*amoA* gene abundances, but the +I treatment did not affect them (Figure 2i). Gene abundances of AOB-*amoA* were comparable among the four treatments, except for the +N treatment at 630 d (Figure 2ii). The *hao* gene abundances in the +N and +I+N treatments were generally higher than those in the control treatment, while there were no significant differences between the +I and control treatments (Figure 2iii). Soil *nxrB* gene abundances ranged from 1.23 × 10^6 to 1.63 × 10^6 copies g^{-1}, with minimal variation observed among the control, +N, +I and +I+N treatments (Figure 2iv, Supplementary Table S3). The gene abundances of *narG*, *nirS* and *nirK* were in the range of 5.05 × 10^5 to 1.71 × 10^6 copies g^{-1}, 7.54 × 10^7 to 1.58 × 10^8 copies g^{-1} and 7.55 × 10^7 to 2.53 × 10^8 copies g^{-1}, respectively. These

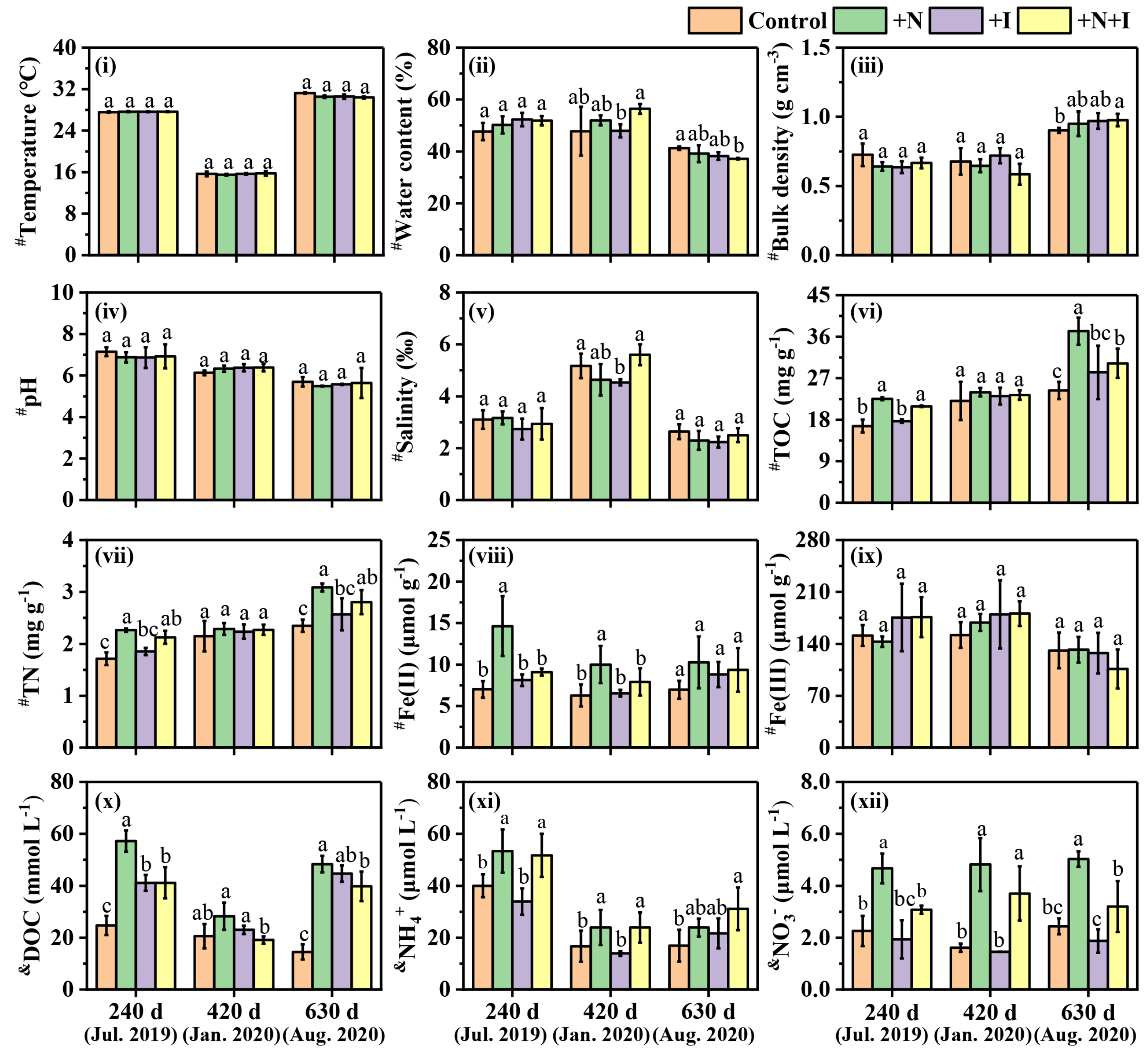

FIGURE 1
The effects of nitrogen addition and inundation increase as well as their interactions on the geochemical properties of soil (#) and porewater (&) (**i**: Temperature, **ii**: Water content, **iii**: Bulk density, **iv**: pH, **v**: Salinity, **vi**: TOC, **vii**: TN, **viii**: Fe(II), **ix**: Fe(III), **x**: DOC, **xi**: NH4+, **xii**: NO3-). Control: control treatments, +N: nitrogen addition treatments; +I: inundation increase treatments; +N+I: combined nitrogen addition and inundation increase treatments. Different lowercase letters indicate significant differences (p < 0.05) among different treatments on the same sampling date.

values were generally higher in the +N and +I+N treatments compared to the control and +I treatments, with no significant differences observed between the latter two (Figures 2v–vii). The +I +N treatment significantly increased the *nosZ* gene abundances, while the +N and +I treatments did not affect their abundances (Figure 2viii). At 240 d (Jul. 2019) and 420 d (Jan. 2020), the (*nirS* +*nirK*)/*nosZ* levels in the +N and +I+N treatments were generally higher than those in the control and +I treatments. However, by 630 d (Aug. 2020), the (*nirS*+*nirK*)/*nosZ* was highest in the +N treatment, followed by the control and +N+I treatments, and lowest in the +I treatment (Figure 2ix).

3.3 Soil N_2O dynamics

Soil $N_2O_{Net\ emission}$ varied from 0.42 to 2.53 nmol g^{-1} h^{-1}, and the +N treatment led to a significant increase in net N_2O emissions, but the +I and +I+N treatments generally did not change them, except for the +I+N treatment at 240 d (Jul. 2019) (Figure 3i). Soil $N_2O_{Gross\ production}$ and $N_2O_{Gross\ consumption}$ were in the range of 1.42 to 8.31 nmol g^{-1} h^{-1} and 0.83 to 6.48 nmol g^{-1} h^{-1}, respectively, and both values in the +N and +I+N treatments were significantly higher than those in the control and +I treatments, but no obvious differences were observed between the latter two (Figures 3ii, iii).

10.3389/fmars.2025.1751567

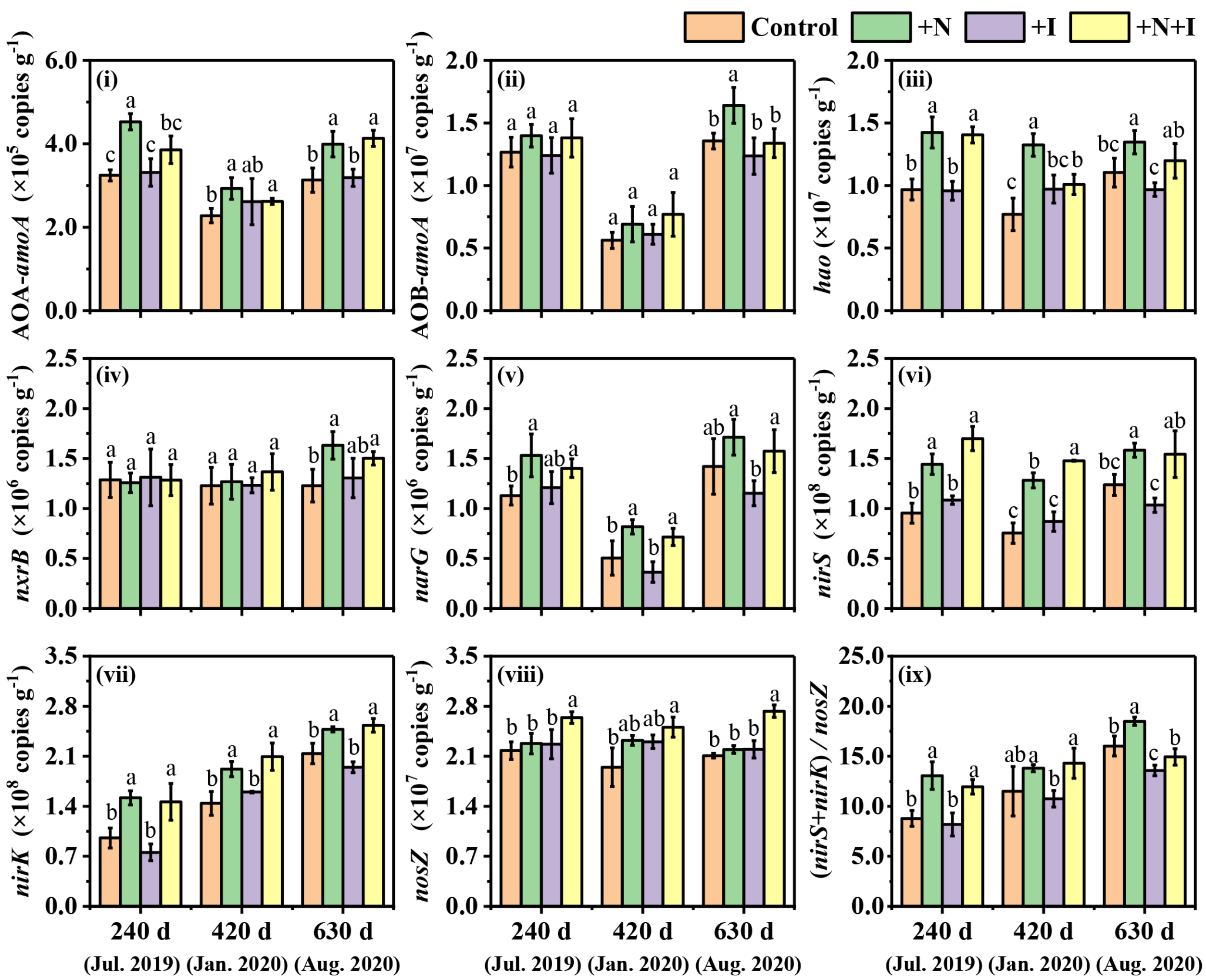

FIGURE 2
The effects of nitrogen addition and inundation increase as well as their interactions on gene abundances involved N_2O production and consumption processes (**i**: AOA-amoA, **ii**: AOB-amoA, **iii**: hao, **iv**: nxrB, **v**: narG, **vi**: nirS, **vii**: nirK, **viii**: nosZ, **ix**: (nirS+nirK)/nosZ). Control: control treatments, +N: nitrogen addition treatments; +I: inundation increase treatments; +N+I: combined nitrogen addition and inundation increase treatments. Different lowercase letters indicate significant differences (*p* < 0.05) among different treatments on the same sampling date.

The $N_2O_{Consumption\ proportion}$ (60.02 – 80.39%) was generally higher in the +I+N treatment than in the control, +N and +I treatments, although some differences were not significant (Figure 3iv). In addition, the $N_2O_{Net\ emission}$, $N_2O_{Gross\ production}$ and $N_2O_{Gross\ consumption}$ at 240 d (Jul. 2019) and 630 d (Aug. 2020) were higher than those at 420 d (Jan. 2020), while there were no significant differences for $N_2O_{Consumption\ proportion}$ among different sampling dates (Figure 3, Supplementary Table S4).

3.4 Environmental variables affecting N_2O dynamics

The RDA results showed that RDA1 and RDA2 accounted for approximately 68.85% and 11.34% of the variations in N_2O dynamics, respectively (Figure 4). Soil samples in +N and +N+I treatments were clearly separated from those in control and +I treatments along RDA1 and RDA2, while the samples in the latter two treatments were not distinctly separated (Figure 4). Correlation analysis showed that soil $N_2O_{Net\ emission}$, $N_2O_{Gross\ production}$ and $N_2O_{Gross\ consumption}$ were all significantly correlated with temperature, salinity, Fe(II), Fe(III), DOC, NH_4^+, NO_3^-, AOA-*amoA*, AOB-*amoA*, *hao*, *narG*, and *nirS*, and $N_2O_{Gross\ production}$ and $N_2O_{Gross\ consumption}$ were also tightly related to (*nirS*+*nirK*)/*nosZ* (Figure 4, Table 1). Soil $N_2O_{Consumption\ proportion}$ was only associated with *nirS* and *nosZ* abundances (Figure 4, Table 1). The random forest (RF) analysis revealed that salinity, DOC, AOA-*amoA*, AOB-*amoA* and *narG* were very important variables for $N_2O_{Net\ emission}$, while AOA-*amoA*, AOB-*amoA*, *narG* and *nirS* were identified as crucial factors influencing $N_2O_{Gross\ production}$ and N_2O_{Gross}

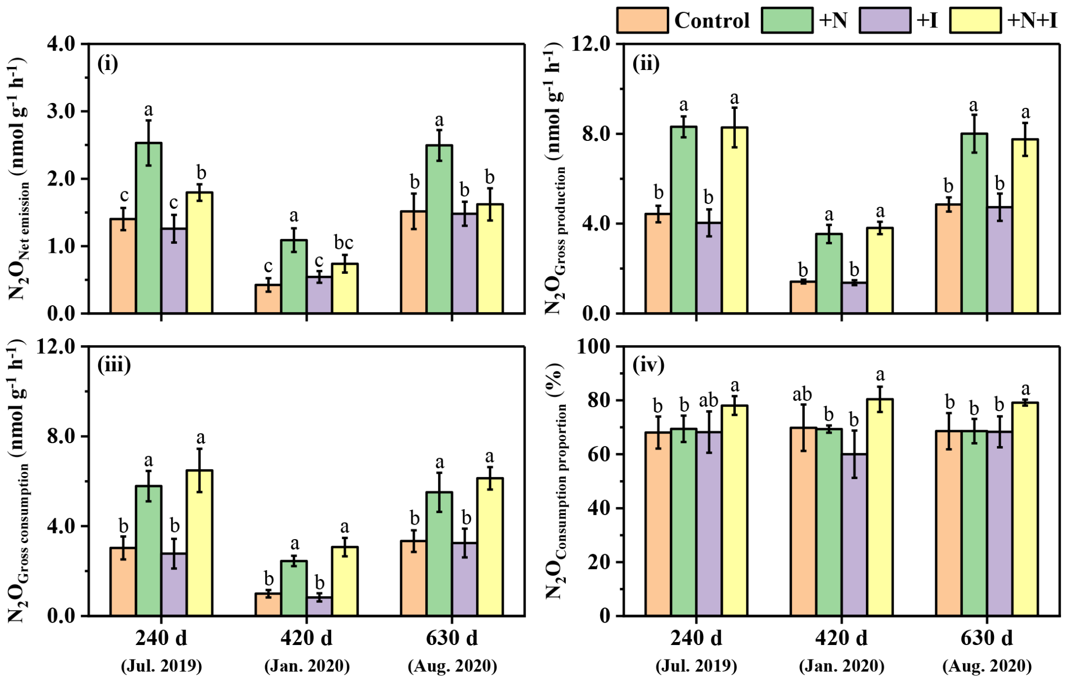

FIGURE 3
The effects of nitrogen addition and inundation increase as well as their interactions on the soil N_2O dynamics (**i**: N_2O Net emission, **ii**: N_2O Gross producion, **iii**: N_2O Gross consumption, **iv**: N_2O consumption proportion). Control: control treatments, +N: nitrogen addition treatments; +I: inundation increase treatments; +N+I: combined nitrogen addition and inundation increase treatments. Different lowercase letters indicate significant differences (p < 0.05) among different treatments on the same sampling date.

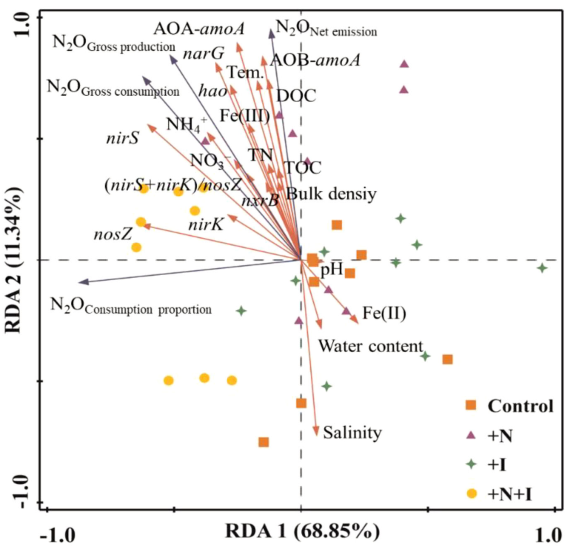

FIGURE 4
Ordination diagram showing the results of RDA of N_2O dynamics, geochemical properties of soil and porewater, as well as associated gene abundances. ($N_2O_{Net\ emission}$: net N_2O emission rates, $N_2O_{Gross\ production}$: gross N_2O production rates, $N_2O_{Gross\ consumption}$: gross N_2O consumption rates, $N_2O_{Consumption\ proportion}$: N_2O consumption proportion, Tem.: Temperature).

TABLE 1 Spearman correlation analyses of soil N_2O dynamics with geochemical properties and gene abundance.

Parameters	$N_2O_{Net\ emission}$	$N_2O_{Gross\ production}$	$N_2O_{Gross\ consumption}$	$N_2O_{Consumption\ proportion}$
Temperature	0.64**	0.69**	0.63**	0.11
Water content	-0.29	-0.35*	-0.30	-0.09
Bulk density	0.28	0.35*	0.32	0.13
pH	-0.03	-0.07	-0.07	-0.07
Salinity	-0.65**	-0.63**	-0.54**	0.02
TOC	0.22	0.206	0.201	0.08
TN	0.28	0.306	0.32	0.13
Fe(II)	0.56**	0.59**	0.59**	0.22
Fe(III)	-0.37*	-0.43**	-0.38*	-0.09
DOC	0.68**	0.61**	0.55**	0.02
NH_4^+	0.55**	0.63**	0.63**	0.32
NO_3^-	0.48**	0.46**	0.47**	0.21
AOA-*amoA*	0.89**	0.84**	0.76**	0.06
AOB-*amoA*	0.85**	0.76**	0.68**	-0.04
hao	0.68**	0.66**	0.65**	0.17
nxrB	0.24	0.29	0.32	0.17
narG	0.87**	0.87**	0.81**	0.17
nirS	0.65**	0.71**	0.75**	0.46**
nirK	0.19	0.26	0.32	0.28
nosZ	0.06	0.22	0.35*	0.52**
(*nirS*+*nirK*)/*nosZ*	0.32	0.35*	0.374*	0.199

* Significant at $p < 0.05$, ** Significant at $p < 0.01$, $n = 36$.

$_{consumption}$ (Figures 5i–iii). In addition, NH_4^+ and *nosZ* abundance were found to be the most dominant factors for $N_2O_{Consumption\ proportion}$ (Figure 5iv).

4 Discussion

4.1 Effects of nitrogen enrichment and inundation increase on N_2O dynamics

Nitrogen loading enhancement and inundation increase caused by anthropogenic activities and sea-level rise are considered as the important drivers altering biogeochemical processes in estuarine and coastal wetlands (Saintilan et al., 2020; Peng et al., 2021). Our newly revealed details show that these two drivers and their interactions affect soil N_2O dynamics to varying extents, which improves our comprehension of N_2O cycles in the context of global environmental change. In this study, $N_2O_{Net\ emission}$ in the +N treatment on three different sampling dates was significantly higher than that in the control treatment (Figure 3i), indicating that nitrogen enrichment promoted N_2O emission. This result was mainly attributed to the fact that nitrogen ($NaNO_3$ and NH_4Cl) input increased NH_4^+ and NO_3^- availabilities (Figures 1xi, xii), which provided enough substrates for nitrification and denitrification, two important N_2O production processes (Quick et al., 2019; Li et al., 2023). Meanwhile, nitrogen input can accelerate plant growth and increase organic carbon contents through a larger return of litter to the soil (Henneron et al., 2020; Zhang et al., 2022). Higher organic carbon is favorable for nitrification and denitrification processes as well as related N_2O production (Butterbach-Bahl et al., 2013; Ji et al., 2015; Jiang et al., 2025). Indeed, soil TOC contents and porewater DOC concentrations in the +N treatment were generally higher than those in the control treatment (Figures 1vi, x), which may also contribute to an increase in net N_2O emissions in the former. The results of correlation and RDA analysis in the present study also supported these inferences (Figure 4, Table 1). Theoretically, N_2O emissions in natural ecosystems are mainly dependent on their production and consumption, and how these two processes balance will determine the ultimate emissions (Yang and Silver, 2016; Chen et al., 2023). Here, we applied the C_2H_2 inhibition method to estimate gross N_2O production and consumption rates, and found that both $N_2O_{Gross\ production}$ and $N_2O_{Gross\ consumption}$ significantly increased in the +N treatment compared to the control treatment (Figures 3ii, iii). However, unlike gross N_2O production and consumption rates, the $N_2O_{Consumption\ proportion}$ was not higher in the

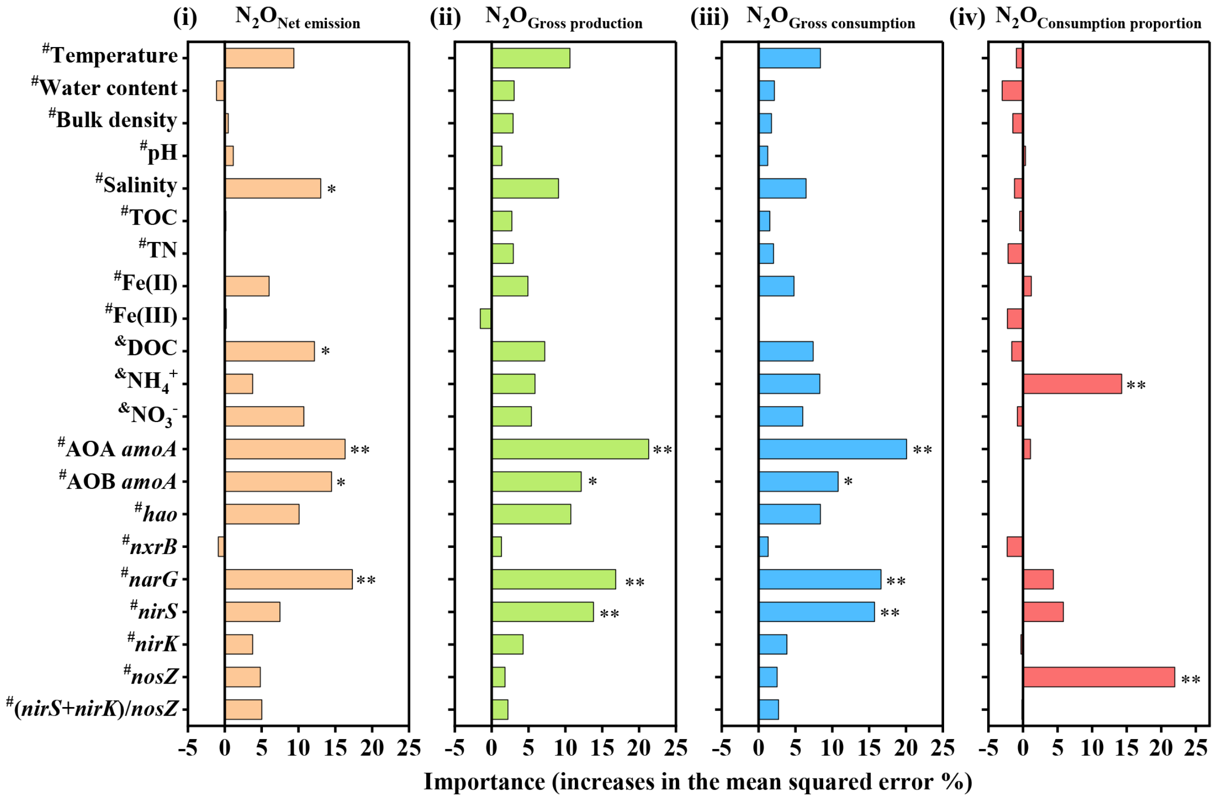

FIGURE 5
Random forest predictor importance, as determined by percent increase in mean square error (MSE) of N2O dynamics (**i**: $N_2O_{Net\ emission}$, **ii**: $N_2O_{Gross\ producition}$, **iii**: $N_2O_{Gross\ consumption}$, **iv**: $N_2O_{consumption\ proportion}$). Asterisks indicate levels of significance (p < 0.05; *p < 0.01).

+N treatment compared to the control treatment (Figure 3iv). Therefore, we attribute the increased N_2O emission under +N treatment primarily to enhanced gross N_2O production, rather than to a change in N_2O consumption. In addition, N_2O dynamics are also regulated by microbial activities, and gene abundances associated with N_2O production and consumption can serve as proxies for characterizing the magnitude of N_2O emission (Aamer et al., 2020; Lin et al., 2022). In this study, most of the gene abundances involved in N_2O production (AOA-*amoA*, *hao*, *narG*, *nirS* and *nirK*) were higher in the +N treatment compared to the control treatment, while *nosZ* abundance, the N_2O reductase gene, did not differ between the two treatments (Figure 2), which further confirmed the aforementioned results. Although nitrogen enrichment has been widely proven to stimulate N_2O emission in estuarine and coastal wetlands (Zhang et al., 2013; Martin et al., 2018; Quick et al., 2019; Li et al., 2023), our results highlighted that gross N_2O production rather than consumption was the direct driver for the increase of N_2O emission in such environments.

In the present study, there were no significant differences in $N_2O_{Net\ emission}$ between the +I and control treatments on three sampling dates (Figure 3i), indicating that inundation increase alone did not change N_2O emission. Generally, increased inundation caused by sea-level rise can elevate soil salinity and thus affect element biogeochemical processes (Chambers et al., 2014; Mills et al., 2021). However, no obvious variations in soil salinity were observed between the +I and control treatments (Figure 1v), which can be attributed to the fact that we only simulated inundation increase without accompanying high salinity saltwater intrusion. This may be one of the reasons for the comparable N_2O emissions in both the +I and control treatments. In addition, increased inundation can impede N_2O diffusion out of soil, and allow more N_2O to be reduced, thereby decreasing its emission (Chapuis-Lardy et al., 2007; Yang and Silver, 2016). Surprisingly, this phenomenon also did not occur in the +I treatment (Figure 3i). In our study, $N_2O_{Gross\ production}$ in the +I treatment was relatively low, as with the control treatment (Figure 3ii), and we deduced that increased inundation may not be enough to affect N_2O reduction by impeding gaseous diffusion in environments with lower N_2O production. That is to say, N_2O reduction is only influenced by the increased inundation when its production reaches a certain level. The results of the +N and +N+I treatments strongly supported this hypothesis. Specifically, gross N_2O production in both the +N and +N+I treatments was relatively high, but net N_2O emissions in the latter were significantly lower due to a higher proportion of N_2O consumption (Figure 3). It appears that increased inundation played a vital role in regulating N_2O reduction under higher N_2O production conditions. Previous studies noted that the *nosZ* gene is an important indicator in reflecting N_2O reduction in natural ecosystems (Park et al., 2017; Aamer et al., 2020; Kim et al., 2022). In theory, higher N_2O production and slower N_2O diffusion in the +N+I treatment can provide N_2O substrates for N_2O reduction microorganisms and increase *nosZ* gene abundance (Chapuis-Lardy

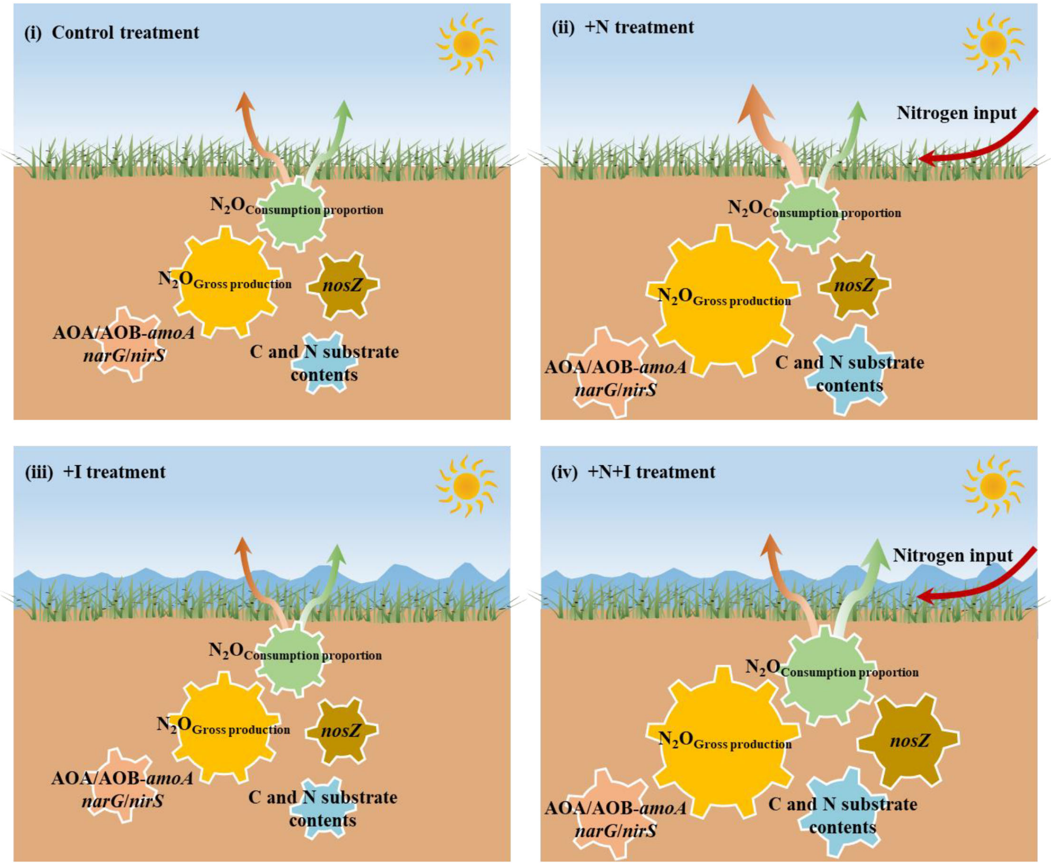

FIGURE 6
A conceptual schematic for the N_2O dynamics and key influencing factors under the control **(i)**, +N **(ii)**, +I **(iii)**, and +N+I **(iv)** treatments. The area ofpolygons and the thickness of the arrows represent the relative importance of variables. Graphics of the sun and flora from Integration and Application Network (ian.umces.edu/media-library), licensed under Attribution-ShareAlike 4.0 International (CC BY-SA 4.0).

et al., 2007; Quick et al., 2019). Indeed, *nosZ* abundance in the +N+I treatment was significantly higher than that in other treatments (Figure 2viii), which further confirmed the above-mentioned perspective. The importance of the *nosZ* gene in N_2O reduction was also supported by the results of correlation and random forest analysis (Table 1 and Figure 5). Additionally, the (nirS+nirK)/nosZ ratio denotes the balance between N_2O production and consumption, with a higher ratio favoring N_2O accumulation and emission and a lower ratio enhancing reduction and limiting release (Lin and Lin, 2022), thereby helping to explain the observed N_2O. It has been reported that N_2O can be a more favorable electron acceptor in the denitrification process under the lower NO_3^- conditions (Murray et al., 2015). In this study, NO_3^- concentrations in porewater were generally lower in +N+I treatment than in +N treatment (Figure 1xii), and this may be another important reason why +N+I treatment had a higher N_2O consumption proportion. Similar temporal variations in N_2O dynamics were observed in the control, +N, +I, and +N+I treatments. Soil gross N_2O production and consumption, as well as ultimate emission rates at 240 d and 630 d were significantly higher than those at 420 d (Figure 3), which could be explained by the changes in temperature. Previous studies have reported that N_2O cycles tend to increase with increasing temperature in natural environments (Butterbach-Bahl et al., 2013; Gao et al., 2022). Clearly, soil temperatures at 240 d (Jul. 2019) and 630 d (Aug. 2020) were larger than those at 420 d (Jan. 2020) due to the seasonal features. In addition, Additionally, salinity may regulate N_2O dynamics, as higher levels can inhibit both its production and emission to some extent (Lin et al., 2025), which also helps explain the lower N_2O emissions at the 420 d. Hence, nitrogen input and inundation increase did not alter the seasonal changes of soil N_2O dynamics.

4.2 Environmental implications and future outlook

Over the past several decades, global reactive nitrogen levels have rapidly increased due to intensive human activities (Canfield et al., 2010; Peng et al., 2021). Wherein, approximately 20 – 30% of this reactive nitrogen is transported into estuarine and coastal zones through hydrological and atmospheric pathways, leading to a significant increase in nitrogen loading (Chen et al., 2016; Li et al., 2023). In addition, sea-level rise due to continued global warming is likely to pose a grave threat to estuarine and coastal ecosystems (Nicholls et al., 2021; Lorenz et al., 2023). Global mean sea-level rise is estimated at 0.37 – 0.86 m and 0.98 – 1.88 m by 2150, respectively, in low and high global greenhouse gas emission scenarios (IPCC, 2021).

Overall, nitrogen loading enhancement and sea-level rise are the typical environmental concerns in estuarine and coastal wetlands, which affect element biogeochemical cycling and ecosystem health (Wang et al., 2018; Liu et al., 2022). In our study, we explored the changes in N_2O dynamics after nitrogen input and inundation increase in an attempt to reveal their potential response to nitrogen loading enhancement and sea-level rise. The results are significant for gaining insight into the global N_2O budget and the climate feedback linked to nitrogen loading enhancement and sea-level rise (Yang and Silver, 2016; Tian et al., 2020). Here, we proposed a conceptual framework for understanding N_2O dynamics affected by the aforementioned drivers (Figure 6), offering a new perspective on grasping N_2O emissions in the context of global environmental change. The present study indicated that nitrogen input (+N treatment) significantly increased N_2O emission by stimulating gross N_2O production (Figures 6i, ii). Furthermore, our findings also highlighted the importance of increasing inundation in alleviating the nitrogen enrichment effects on N_2O emission (+N+I treatment), although inundation alone (+I treatment) did not change N_2O dynamics (Figures 6iii, iv). It follows that in nitrogen-rich environments, increased inundation caused by sea-level rise may enhance the ability of soil to act as an N_2O sink and further decrease N_2O emissions. These results implied that N_2O emissions in estuarine and coastal wetlands simultaneously experiencing nitrogen loading enhancement and sea-level rise may not have obvious changes. Hence, suitable inundation may help to mitigate N_2O emissions in such ecosystems under conditions of high nitrogen loading. This phenomenon may be common in estuarine and coastal wetlands but has often been overlooked. Notably, our weir design mainly focused on the effects of inundation duration on N_2O dynamics under a sea level rise scenario, but does not consider inundation water duration and frequency. In addition, the simulation experiment in our study was conducted at a single location, perhaps limiting the comprehensive understanding of the effects of sea-level rise at a larger ecosystem level. We recommend that future studies should be carried out by *in situ* soil/plant translocation experiments on larger spatial scales. Nevertheless, our findings highlighted the importance of understanding the controls on the specific processes that lead to N_2O consumption. This understanding is crucial for improving predictions of how net N_2O emissions in estuarine and coastal wetlands will be affected by nitrogen loading enhancement and sea-level rise.

5 Conclusions

Our study provides an early insight into the effects of nitrogen loading enhancement and inundation increase caused by intensive human activity and sea-level rise on soil N_2O dynamics in estuarine and coastal wetlands. Nitrogen input significantly stimulated N_2O emission by increasing gross N_2O production, and N_2O consumption did not change this pattern. The N_2O production and consumption, as well as ultimate emission, were not influenced by inundation increase alone. Increased inundation under nitrogen input conditions alleviated N_2O accumulation due to the higher N_2O consumption proportion. Soil carbon and nitrogen substrate contents, as well as gene abundances associated with N_2O production and consumption, were found to be the crucial factors controlling the variations in N_2O dynamics. Overall, our findings showed the importance of increased inundation caused by sea-level rise in mitigating N_2O emissions in nitrogen-rich environments, which provided the scientific basis for the management of estuarine coastal wetlands.

Data availability statement

The original contributions presented in the study are included in the article/Supplementary Material. Further inquiries can be directed to the corresponding author.

Author contributions

DG: Methodology, Writing – review & editing, Software, Investigation, Writing – original draft, Formal analysis, Conceptualization, Funding acquisition. YZ: Formal analysis, Writing – review & editing, Software. JH: Project administration, Writing – review & editing, Formal analysis, Methodology, Validation, Software, Investigation, Supervision, Funding acquisition.

Funding

The author(s) declared that financial support was received for this work and/or its publication. This work was supported by the Natural Science Foundation of China (grant number: 42206237) and the Fujian Provincial Natural Science Foundation of China (grant numbers: 2024J01463; 2024J01446). It was also funded by the Public Welfare Project of Fujian Science and Technology Department (2022R1002007).

Acknowledgments

We thank Prof. Min Luo for his guidance and assistance during the experiments, and we also thank the Integration and Application Network for providing the symbols (ian.umces.edu/symbols/).

Conflict of interest

The author(s) declared that this work was conducted in the absence of any commercial or financial relationships that could be construed as a potential conflict of interest.

The handling editor XL declared a past co-authorship with the authors DG and JH.

Generative AI statement

The author(s) declared that generative AI was not used in the creation of this manuscript.

Any alternative text (alt text) provided alongside figures in this article has been generated by Frontiers with the support of artificial intelligence and reasonable efforts have been made to ensure accuracy, including review by the authors wherever possible. If you identify any issues, please contact us.

Publisher's note

All claims expressed in this article are solely those of the authors and do not necessarily represent those of their affiliated organizations, or those of the publisher, the editors and the reviewers. Any product that may be evaluated in this article, or claim that may be made by its manufacturer, is not guaranteed or endorsed by the publisher.

Supplementary material

The Supplementary Material for this article can be found online at: https://www.frontiersin.org/articles/10.3389/fmars.2025.1751567/full#supplementary-material

References

Aamer, M., Shaaban, M., Hassan, M. U., Huang, G. Q., Liu, Y., Tang, H. Y., et al. (2020). Biochar mitigates the N_2O emissions from acidic soil by increasing the *nosZ* and *nirK* gene abundance and soil pH. *J. Environ. Manage.* 255, 109891. doi: 10.1016/j.jenvman.2019.109891

Bi, R. Y., Xu, X. T., Wang, B. X., Jiao, Y., Zhang, Q. Q., and Xiong, Z. Q. (2024). Evidence of complete ammonia-oxidizing microbial communities and their contribution to N_2O emissions in typical vegetable fields across China. *Soil Biol. Biochem.* 194, 109423. doi: 10.1016/j.soilbio.2024.109423

Butterbach-Bahl, K., Baggs, E. M., Dannenmann, M., Kiese, R., and Zechmeister-Boltenstern, S. (2013). Nitrous oxide emissions from soils: how well do we understand the processes and their controls? *Philos. Trans. R. Soc. B-Biological Sci.* 368, 20130122. doi: 10.1098/rstb.2013.0122

Canfield, D. E., Glazer, A. N., and Falkowski, P. G. (2010). The evolution and future of Earth's nitrogen cycle. *Science.* 330, 192e196. doi: 10.1126/science.1186120

Chambers, L. G., Davis, S. E., Troxler, T., Boyer, J. N., Downey-Wall, A., and Scinto, L. J. (2014). Biogeochemical effects of simulated sea level rise on carbon loss in an Everglades mangrove peat soil. *Hydrobiologia.* 726, 195–211. doi: 10.1007/s10750-013-1764-6

Chapuis-Lardy, L., Wrage, N., Metay, A., Chotte, J. L., and Bernoux, M. (2007). Soils, a sink for N_2O? *A review. Global Change Biol.* 13, 1–17. doi: 10.1111/j.1365-2486.2006.01280.x

Chen, F., Hou, L., Liu, M., Zheng, Y., Yin, G., Lin, X., et al. (2016). Net anthropogenic nitrogen inputs (NANI) into the Yangtze River basin and the relationship with riverine nitrogen export. *J. Geophysical Research-Biogeosciences.* 121, 451e465. doi: 10.1002/2015JG003186

Chen, X., Zhang, S. B., Liu, J., Wang, J. F., Xin, Y., Sun, S. Y., et al. (2023). Tracing microbial production and consumption sources of N_2O in rivers on the Qinghai-Tibet Plateau via isotopocule and functional microbe analyses. *Environ. Sci. Technol.* 57, 7196–7205. doi: 10.1021/acs.est.3c00950

Cherry, J. A., Ramseur, G. S. J., Sparks, E. L., and Cebrian, J. (2015). Testing sea-level rise impacts in tidal wetlands: a novel in *situ* approach. *Methods Ecol. Evol.* 6, 1443–1451. doi: 10.1111/2041-210X.12441

Dieleman, W. I. J., Vicca, S., Dijkstra, F. A., Hagedorn, F., Hovenden, M. J., Larsen, K. S., et al. (2012). Simple additive effects are rare: a quantitative review of plant biomass and soil process responses to combined manipulations of CO_2 and temperature. *Global Change Biol.* 18, 2681–2693. doi: 10.1111/j.1365-2486.2012.02745.x

Feng, J., Zeng, X., Zhang, Q., Zhou, X., Liu, Y., and Huang, Q. (2021). Soil microbial trait-based strategies drive metabolic efficiency along an altitude gradient. *ISME Commun.* 1, 71. doi: 10.1038/s43705-021-00076-2

Gao, D. Z., Hou, L. J., Liu, M., Zheng, Y. L., Yin, G. Y., and Niu, Y. H. (2022). N_2O emission dynamics along an intertidal elevation gradient in a subtropical estuary: Importance of N_2O consumption. *Environ. Res.* 205, 112432. doi: 10.1016/j.envres.2021.112432

Gao, D. Z., Li, X. F., Lin, X. B., Wu, D. M., Jin, B. S., Huang, Y. P., et al. (2017). Soil dissimilatory nitrate reduction processes in the *Spartina alterniflora* invasion chronosequences of a coastal wetland of southeastern China: Dynamics and environmental implications. *Plant Soil.* 421, 383–399. doi: 10.1007/s11104-017-3464-x

Henneron, L., Kardol, P., Wardle, D. A., Cros, C., and Fontaine, S. (2020). Rhizosphere control of soil nitrogen cycling: a key component of plant economic strategies. *New Phytol.* 228, 1269–1282. doi: 10.1111/nph.16760

Hu, M., Wilson, B. J., Sun, Z., Ren, P., and Tong, C. (2016). Effects of the addition of nitrogen and sulfate on CH_4 and CO_2 emissions, soil, and pore water chemistry in a high marsh of the Min River estuary in southeastern China. *Sci. Total Environ.* 579, 292–304. doi: 10.1016/j.scitotenv.2016.11.103

IPCC (2021). "Summary for policymakers," in *Climate change 2021: The physical science basis*. Eds. V. Masson-Delmotte, P. Zhai, A. Pirani, S. L. Connors, C. Péan, S. Berger, et alContribution of Working Group I to the Sixth Assessment Report of the Intergovernmental Panel on Climate Change (Cambridge, United Kingdom and New York, NY, USA: Cambridge University Press).

Ji, Q. X., Babbin, A. R., Jayakumar, A., Oleynik, S., and Ward, B. B. (2015). Nitrous oxide production by nitrification and denitrification in the Eastern Tropical South Pacific oxygen minimum zone. *Geophysical Res. Lett.* 42, 10755–10764. doi: 10.1002/2015GL066853

Jia, J., Bai, J. H., Wang, W., Yin, S., Zhang, G. L., Zhao, Q. Q., et al. (2020). Salt stress alters the short-term responses of nitrous oxide emissions to the nitrogen addition in salt-affected coastal soils. *Sci. Total Environ.* 742, 140124. doi: 10.1016/j.scitotenv.2020.140124

Jiang, Q. Y., Cao, L., Han, Y. C., Li, S. J., Zhao, R., Zhang, X. L., et al. (2025). Cold seeps are potential hotspots of deep-sea nitrogen loss driven by microorganisms across 21 phyla. *Nat. Commun.* 16, 1646. doi: 10.1038/s41467-025-56774-1

Jones, S. F., Stagg, C. L., Krauss, K. W., and Hester, M. W. (2018). Flooding alters plant-mediated carbon cycling independently of elevated atmospheric CO_2 concentrations. *J. Geophysical Research-Biogeosciences.* 123, 1976–1987. doi: 10.1029/2017JG004369

Kim, D. D., Han, H., Yun, T., Song, M. J., Terada, A., Lauren, M., et al. (2022). Identification of *nosZ*-expressing microorganisms consuming trace N_2O in microaerobic chemostat consortia dominated by an uncultured Burkholderiales. *ISME J.* 16, 2087–2098. doi: 10.1038/s41396-022-01260-5

Kostka, J. E., and Luther, G. W.III (1994). Partitioning and speciation of solid phase iron in saltmarsh sediments. *Geochimica Cosmochimica Acta.* 58, 1701–1710. doi: 10.1016/0016-7037(94)90531-2

Lenstra, W. K., Hermans, M., Séguret, M. J., Witbaard, R., Severmann, S., Behrends, T., et al. (2021). Coastal hypoxia and eutrophication as key controls on benthic release and water column dynamics of iron and manganese. *Limnology Oceanography.* 66, 807–826. doi: 10.1002/lno.11644

Lewis, D., Brown, J., and Jimenez, K. (2014). Effects of flooding and warming on soil organic matter mineralization in Avicennia germinans mangrove forests and Juncus roemerianus salt marshes. *Estuar. Coast. Shelf Sci.* 139, 11–19. doi: 10.1016/j.ecss.2013.12.032

Li, X., Gao, D., Hou, L., and Liu, M. (2019). Salinity stress changed the biogeochemical controls on CH_4 and N_2O emissions of estuarine and intertidal sediments. *Sci. Total Environ.* 652, 593–601. doi: 10.1016/j.scitotenv.2018.10.294

Li, X. F., Gao, D. Z., Li, Y., Zheng, Y. L., Dong, H. P., Liang, X., et al. (2023). Increased nitrogen loading facilitates nitrous oxide production through fungal and chemodenitrification in estuarine and coastal sediments. *Environ. Sci. Technol.* 57, 2660–2671. doi: 10.1021/acs.est.2c06602

Li, X. F., Sardans, J., Qi, M. T., Ni, X. Y., Zhang, M. F., Penuelas, J., et al. (2022). Nitrous oxide concentration and flux in Min River Basin of southeast China: Effects of land use, stream order and water variables. *J. Hydrology.* 614, 128507. doi: 10.1016/j.jhydrol.2022.128507

Lin, G. M., and Lin, X. B. (2022). Bait input altered microbial community structure and increased greenhouse gases production in coastal wetland sediment. *Water Res.* 218, 118520. doi: 10.1016/j.watres.2022.118520

Lin, H., Yuan, Q. Y., Yu, Q. G., Chen, Z. M., and Ma, J. W. (2022). Plants mitigate nitrous oxide emissions from antibiotic-contaminated agricultural soils. *Environ. Sci. Technol.* 56, 4950–4960. doi: 10.1021/acs.est.1c06508

Lin, X. B., Zhu, B. Q., Peng, Y. Y., Lin, G. M., Sun, D. Y., and Ye, W. W. (2025). Responses of microbial communities and greenhouse gas production to land use change in mangrove wetland sediments. *Limnology Oceanography.* 70, 1210–1225. doi: 10.1002/lno.70028

Liu, B. G., Tong, C., Fang, Y. Y., Vancov, T., Wang, W. Q., Yang, P., et al. (2022). Interactive effects of sea-level rise and nitrogen enrichment on the decay of different plant residues in an oligohaline estuarine marsh. *Estuar. Coast. Shelf Sci.* 270, 107835. doi: 10.1016/j.ecss.2022.107835

Lorenz, M., Arns, A., and Gräwe, U. (2023). How sea level rise may hit you through the backdoor: changing extreme water levels in shallow coastal lagoons. *Geophysical Res. Lett.* 50, e2023GL105512. doi: 10.1029/2023GL105512

Luo, M., Huang, J. F., Zhu, W. Z., and Tong, C. (2019). Impacts of increasing salinity and inundation on rates and pathways of organic carbon mineralization in tidal wetlands: a review. *Hydrobiologia.* 827, 31–49. doi: 10.1007/s10750-017-3416-8

Martin, R. M., Wigand, C., Elmstrom, E., Lloret, J., and Valiela, I. (2018). Long-term nutrient addition increases respiration and nitrous oxide emissions in a New England salt marsh. *Ecol. Evol.* 8, 4958–4966. doi: 10.1002/ece3.3955

Martin, S., Sparks, E. L., Constantin, A. J., Cebrian, J., and Cherry, J. A. (2021). Restoring fringing tidal marshes for ecological function and ecosystem resilience to moderate sea-level rise in the northern gulf of Mexico. *Environ. Management.* 67, 384–397. doi: 10.1007/s00267-020-01410-5

Mills, L., Janeiro, J., and Martins, F. (2021). Effects of sea level rise on salinity and tidal flooding patterns in the Guadiana Estuary. *J. Water Climate Change.* 12, 2933–2947. doi: 10.2166/wcc.2021.202

Moseman-Valtierra, S., Gonzalez, R., Kroeger, K. D., Tang, J., Chao, W. C., Crusius, J., et al. (2011). Short-term nitrogen additions can shift a coastal wetland from a sink to a source of N_2O. *Atmospheric Environ.* 45, 4390–4397. doi: 10.1016/j.atmosenv.2011.05.046

Mou, X., Liu, X., Tong, C., and Sun, G. (2014). Responses of CH_4 emissions to nitrogen addition and *Spartina alterniflora* invasion in Minjiang River estuary, southeast of China. *Chin. Geographical Sci.* 24, 562–574. doi: 10.1007/s11769-014-0692-3

Murray, R. H., Erler, D. V., and Eyre, B. D. (2015). Nitrous oxide fluxes in estuarine environments: response to global change. *Global Change Biol.* 21, 3219–3245. doi: 10.1111/gcb.12923

Nicholls, R. J., Lincke, D., Hinkel, J., Brown, S., Vafeidis, A. T., Meyssignac, B., et al. (2021). A global analysis of subsidence, relative sea-level change and coastal flood exposure. *Nat. Climate Change.* 11, 338–342. doi: 10.1038/s41558-021-00993-z

Park, D., Kim, H., and Yoon, S. (2017). Nitrous oxide reduction by an obligate aerobic bacterium, gemmatimonas aurantiaca strain T-27. *Appl. And Environ. Microbiol.* 83, e00502–e00517. doi: 10.1128/AEM.00502-17

Peng, X., Ji, Q., Angell, J. H., Kearns, P. J., Bowen, J. L., and Ward, B. B. (2021). Long-term fertilization alters nitrous oxide cycling dynamics in salt marsh sediments. *Environ. Sci. Technol.* 55, 10832–10842. doi: 10.1021/acs.est.1c01542

Quick, A. M., Reeder, W. J., Farrell, T. B., Tonina, D., Feris, K. P., and Benner, S. G. (2019). Nitrous oxide from streams and rivers: A review of primary biogeochemical pathways and environmental variables. *Earth-Science Rev.* 191, 224–262. doi: 10.1016/j.earscirev.2019.02.021

Ravishankara, A. R., Daniel, J. S., and Portmann, R. W. (2009). Nitrous oxide (N_2O): the dominant ozone-depleting substance emitted in the 21st century. *Science.* 326, 123–125. doi: 10.1126/science.1176985

Saintilan, N., Khan, N. S., Ashe, E., Kelleway, J. J., Rogers, K., Woodroffe, C. D., et al. (2020). Thresholds of mangrove survival under rapid sea level rise. *Science* 368, 1118–1121. doi: 10.1126/science.aba2656

Stachelek, J., Kelly, S. P., Sklar, F. H., Coronado-Molina, C., Troxler, T., and Bauman, L. (2018). *In situ* simulation of sea-level rise impacts on coastal wetlands using a flow-through mesocosm approach. *Methods Ecol. Evol.* 9, 1908–1915. doi: 10.1111/2041-210X.13028

Stagg, C., Schoolmaster, D., Krauss, K., Cormier, N., and Conner, W. (2017). Causal mechanisms of soil organic matter decomposition: Deconstructing salinity and flooding impacts in coastal wetlands. *Ecology* 98, 2003–2018. doi: 10.1002/ecy.1890

Ti, C., and Yan, X. (2010). Estimation of atmospheric nitrogen wet deposition in China mainland from based on N emission data. *J. Agro-Environment Sci.* 29, 1606–1611. doi: 10.1360/972010-1322

Tian, H. Q., Xu, R. T., Canadell, J. G., Thompson, R. L., Winiwarter, W., Suntharalingam, P., et al. (2020). A comprehensive quantification of global nitrous oxide sources and sinks. *Nature.* 586, 248–256. doi: 10.1038/s41586-020-2780-0

Toyoda, S., Yoshida, N., and Koba, K. (2017). Isotopocule analysis of biologically produced nitrous oxide in various environments. *Mass Spectrometry Rev.* 36, 135–160. doi: 10.1002/mas.21459

Wang, F. M., Lu, X. L., Sanders, C. J., and Tang, J. W. (2018). Tidal wetland resilience to sea level rise increases their carbon sequestration capacity in United States. *Nat. Commun.* 10, 5733. doi: 10.1038/s41467-019-13800-3

Wang, Y., Peng, Y., Lv, C., Xu, X., Meng, H., Zhou, Y., et al. (2023). Quantitative discrimination of algae multi-impacts on N_2O emissions in eutrophic lakes: Implications for N_2O budgets and mitigation. *Water Res.* 235, 119857. doi: 10.1016/j.watres.2023.119857

Wankel, S. D., Ziebis, W., Buchwald, C., Charoenpong, C., de Beer, D., Dentinger, J., et al. (2017). Evidence for fungal and chemodenitrification based N_2O flux from nitrogen impacted coastal sediments. *Nat. Commun.* 8, 15595. doi: 10.1038/ncomms15595

Yang, P., Lin, Y. X., Yang, H., Tong, C., Zhang, L. H., Lai, D. Y. F., et al. (2024). Spatiotemporal distributions of dissolved N_2O concentration, diffusive N_2O flux and relevant functional genes along a coastal creek in southeastern China. *J. Hydrology.* 637, 131331. doi: 10.1016/j.jhydrol.2024.131331

Yang, W. H., and Silver, W. L. (2016). Gross nitrous oxide production drives net nitrous oxide fluxes across a salt marsh landscape. *Global Change Biol.* 22, 2228–2237. doi: 10.1111/gcb.13203

Yin, C., Fan, X., Yan, G., Chen, H., Ye, M., Ni, L., et al. (2020). Gross N_2O production process, not consumption, determines the temperature sensitivity of net N_2O emission in arable soil subject to different longterm fertilization practices. *Front. Microbiol.* 11, 745. doi: 10.3389/fmicb.2020.00745

Zhang, Y., Wang, L., Xie, X., Huang, L., and Wu, Y. (2013). Effects of invasion of *Spartina alterniflora* and exogenous N deposition on N_2O emissions in a coastal salt marsh. *Ecol. Eng.* 58, 77–83. doi: 10.1016/j.ecoleng.2013.06.011

Zhang, L., Wang, L., Yin, K., Lü, Y., Yang, Y., and Huang, X. (2014). Spatial and seasonal variations of nutrients in sediment profiles and their sediment-water fluxes in the Pearl River Estuary, Southern China. *J. Earth Sci.* 25, 197–206. doi: 10.1007/s12583-014-0413-y

Zhang, X. L., Yao, C., Zhang, B. S., Gong, J., Wang, G. Y., Zhao, J. M., et al. (2023). Response of benthic nitrates reduction processes and associated microbial communities to coastal hypoxia. *Environ. Sci. Technol.* 57, 15014–15025. doi: 10.1021/acs.est.3c03994

Zhang, W. L., Zeng, C. S., Tong, C., Zhai, S. J., Lin, X., and Gao, D. Z. (2015). Spatial distribution of phosphorus speciation in marsh sediments along a hydrologic gradient in a subtropical estuarine wetland, China. *Estuar. Coast. Shelf Sci.* 154, 30–38. doi: 10.1016/j.ecss.2014.12.023

Zhang, L. W., Zhao, L. J., Yi, H. P., Lan, S. Q., Chen, L., and Han, G. X. (2022). Nitrogen addition alters plant growth in China's Yellow River Delta coastal wetland through direct and indirect effects. *Front. Plant Sci.* 13, 1016949. doi: 10.3389/fpls.2022.1016949